The Chemist
Journal of the American Institute of Chemists

# Synthesis, Evaluation of Antimicrobial Activity, and Docking Study of Schiff Base-Metronidazole Derivatives

**Aya Yaseen Mahmood Alabdali[1*], Maha Salih Hussein[2]**

[1]*Department of Pharmacy, Faculty of Pharmacy, The University of Mashreq Baghdad 10023, Iraq*
[2]*Department of Chemistry, College of Education, University of Samarra Samarra 34010, Iraq*
**Corresponding author (E-mail: ayaalabdali563@gmail.com, ayaalabdaly@hotmail.com)*

**Abstract:** In recent years, bacterial infections have increased due to resistance and rising air pollution. Since metronidazole is a key drug for treating many diseases, our research focused on the synthesis and modification of novel Schiff base derivatives of metronidazole. The research involved esterifying the hydroxyl group and reducing the nitro group to prepare a Schiff base from the corresponding ester and a chlorometronidazole derivative. Their structures were characterized using IR, $^{1}H$, and $^{13}C$ NMR spectroscopy. Its antibacterial activity against *Pseudomonas aeruginosa* and *Staphylococcus aureus* was then investigated. Derivatives 3 showed the highest inhibition, with diameters of 21 and 25 mm, respectively. Furthermore, molecular docking predicted the strength and type of binding to the protein with (PDB ID: 3U1Y) against *Pseudomonas aeruginosa* and the protein with (PDB ID:5CDQ) against *Staphylococcus aureus*. Schiff base derivatives 3 showed the highest binding at -7.36, -9.15 kcal/mol, respectively. These results indicate that these new compounds are promising antibacterial agents for the future.

**Key Words:** Metronidazole, Schiff bases, *Pseudomonas aeruginosa*, *Staphylococcus aureus,* docking

## 1. Introduction

Among the most significant global concerns are microbial infections, which pose a major threat to public health and contribute significantly to increased mortality world-wide. Although many fungi, viruses, and parasites play a role in infections, bacteria are the most common cause of infectious disorders. Given that multidrug resistance is a major obstacle to combating infectious bacterial diseases, there is an urgent need to

develop new drug compounds to control microbial infections [1].

Metronidazole is a broad-spectrum antimicrobial used clinically to treat many diseases, including infectious ones [2-3]. Its long-term use is often accompanied by numerous side effects [4-6], so much research focuses on its derivatives with novel structures and potential medical and pharmaceutical applications [7-9].

Schiff bases are an emerging class of organic compounds formed by condensation reactions between aromatic amines and carbonyl compounds (aldehydes and ketones). Schiff base chemistry, or imine chemistry, has recently gained significant traction in modern research, primarily due to the presence of the azomethine bond in their structure, which imparts high chemical stability and physicochemical properties that make them promising candidates for numerous biological and pharmaceutical applications [10-12]. Several studies have indicated that metronidazole Schiff base compounds possess distinctive and significant antimicrobial properties [13-16].

In light of previous observations, and as an extension of research and reports on Schiff-metronidazole bases, the main objective of this study was to develop the efficacy of metronidazole by combining it with a Schiff base to improve its pharmacological and biological efficacy, through modification of the nitro group and the hydroxyl group, as its combination is expected to lead to improved antibacterial activity against *Pseudomonas aeruginosa*; *Staphylococcus aureus*, in addition to improving its safety and efficacy as a novel antimicrobial agent. Finally, the results were strengthened by conducting a molecular simulation study of the new Schiff bases to validate the target compounds' activity.

## 2. Materials and Methods

### Chemicals and Instruments

All chemicals and solvents were supplied by Aldrich. An SMP40 automated instrument was used to measure the melting point, and the results were uncorrected. Infrared spectra were recorded using an FT-IR-8400S spectrometer at the College of Education, Samarra University. Proton and carbon nuclear magnetic resonance spectra were recorded using a Varian spectrometer, 400 MHz, at Gaziantep University, Turkey, using d6-dimethyl sulfoxide (DMSO-d6) as the solvent. Thin-layer chromatography (TLC) was used to track reactions and determine product purity. Fluka (USA) used 0.2 mm fluorescently activated silica gel G, and measurements were performed using various solvents. UV-Vis fluorescence at 254 nm was also used.

### 2-(2-methyl-5-nitro-1H-imidazol-1-yl) ethyl benzoate (Met.b)

Metronidazole benzoat**e** was prepared using the method mentioned in the previous literary method [17] in a hood. Metronidazole (8.5 g, 0.05 mol) was carefully dissolved in 35 ml of pyridine, and a solution of benzoyl chloride (5.8 ml, 0.05 mmol) in 15 ml of pyridine was added dropwise. The mixture was stirred at 25°C

for half an hour, then at room temperature overnight. The precipitate was filtered and washed with water. The compound was re-crystallized in ethanol. Pale Yellow powder, Yield: 77%; m. p. 101-102. IR spectrum, (KBr, ύ=$cm^{-1}$), C-H arom.: 3062, C-H aliph.: 2960, C=O: 1718, $NO_2$ group: 1523,1361. $^1$H NMR (400 MHz, DMSO-$d_6$) δ 8.04 (s, 1H, imidazole), 7.85 (d, $J$ = 7.2 Hz, 2H), 7.65 (t, $J$ = 7.4 Hz, 1H), 7.51 (t, $J$ = 7.7 Hz, 2H), 4.75 (t, $J$ = 5.4 Hz, 2H, C$\underline{H}_2$-O), 4.65 (t, $J$ = 9.9 Hz, 2H, C$\underline{H}_2$-N), 2.47 (s, 3H, C$\underline{H}_3$). $^{13}$C NMR (101 MHz, DMSO) δ 165.27 ($\underline{C}$=O), 151.39 ($\underline{C}$-$NO_2$), 138.55, 133.51, 133.12, 129.02, 128.96, 128.76, 62.87($CH_2$-O), 44.69 ($CH_2$-N), 13.88 ($\underline{C}H_3$). Anal. Calcd. For $C_{13}H_{13}N_3O_4$ (275.26): C, 56.72; H, 4.76; N, 15.27; O; 23.25, Found C, 56.80; H, 4.79; N, 15.32; O; 23.29. LCMS: (ESI$^-$-MS, m/z) Calcd. for $C_{13}H_{13}N_3O_4$ (M-H)$^-$: 275.26, Found: 274.31.

**1-(2-chloroethyl)-2-methyl-5-nitro-1H-imidazole (Met.Cl)**

Metronidazole-chloride was prepared using the method mentioned in the previous literature [18,19] with some modifications. Metronidazole (5.2 g, 0.030 mol) was dissolved in $SOCl_2$ (3 ml, 0.04 mol) with 10 ml of chloroform, then the mixture was refluxed for 4 hours, and then cooled. The mixture was stirred at high speed in a cold bath at 10°C for 2 hours. A yellow precipitate was formed. The precipitate was washed with a small amount of cold ethanol to remove residual solvent and $SOCl_2$.

Dark Yellow powder, Yield: 88%; m. p. 79-80. IR spectrum, (KBr, ύ=$cm^{-1}$), C-H arom.: 3037, C-H aliph.: 2970, $NO_2$ group: 1541,1369, C-Cl: 736. $^1$H NMR (400 MHz, DMSO) δ 8.16 (s, 1H), 4.67 (t, $J$ = 6.0 Hz, 2H), 4.01 (t, $J$ = 5.9 Hz, 2H), 2.53 (s, 3H). $^{13}$C NMR (101 MHz, DMSO) δ 151.90 ($\underline{C}$-$NO_2$), 138.38, 132.88, 50.65, 44.81, 14.17($\underline{C}H_3$). Anal. Calcd. For $C_6H_8ClN_3O_2$ (189.60): C, 38.01; H, 4.25; Cl, 18.70; N, 22.16; O; 16.88 Found C, 38.08; H, 4.29; Cl, 18.79; N, 22.19; O; 16.94. LCMS: (ESI$^-$-MS, m/z) Calcd. for $C_6H_8ClN_3O_2$ (M-H)$^-$: 189.60, Found: 188.73.

**General method of reducing the nitro group of metronidazole benzoate (Met.b) and metronidazole chloride (Met.Cl)**

Met.b or Met.Cl (0.004 mol) was dissolved in 25 ml of ethanol, to which (2.0 g, 0.012 mol) of $Na_2S_2O_4$ solution was added. The mixture was heated and stirred for 3 hours at 40°C, then 6 ml of dilute hydrochloric acid (2N) was added and stirred for 3 hours. The mixture was cooled to room temperature, and the solution was neutralized with 25% sodium hydroxide. The product was extracted with (10 ml) dichloromethane three times, the organic layer was washed with water and dried with sodium sulfate, and the solvent was evaporated with a rotary evaporator to obtain a powder precipitate.

**2-(5-amino-2-methyl-1H-imidazol-1-yl) ethyl benzoate 1**

Yellow powder, Yield: 77%; m. p. 101-102. IR spectrum, (KBr, ύ=$cm^{-1}$), N-$H_2$: 4452,3363, C-H arom.: 3026, C-H aliph.: 2981, C=O: 1714.$^1$H NMR (400 MHz, DMSO) δ 7.94 (d, *J* = 8.0 Hz, 2H), 7.83 (s, 1H, imidazole), 7.63 (t, *J* = 7.8 Hz, 1H), 7.55 (s, 2H, $NH_2$), 7.49 (t, *J* = 7.9 Hz, 2H), 4.75 (t, *J* = 5.4 Hz, 2H, $CH_2$-O), 4.65 (t, *J* = 9.9 Hz, 2H, C$\underline{H}_2$-N), 2.46 (s, 3H, C$\underline{H}_3$). $^{13}$C NMR (101 MHz, DMSO) δ 167.99 (C=O), 153.67 (C-$NH_2$), 146.93, 135.93, 129.14, 127.65, 127.19, 124.76, 124.56, 121.25, 62.02(C$\underline{H}_2$-O), 46.42 (C$\underline{H}_2$-N), 16.50 (C$\underline{H}_3$). Anal. Calcd. For $C_{13}H_{15}N_3O_2$ (245.28): C, 63.66; H, 6.16; N, 17.13; O; 13.05, Found C, 63.70; H, 6.19; N, 17.19; O; 13.07. LCMS: (ESI$^-$-MS, m/z) Calcd. for $C_{13}H_{15}N_3O_2(M-H)^-$: 245.28, Found: 244.32.

**1-(2-chloroethyl)-2-methyl-1H-imidazol-5-amine 2**

Dark Yellow powder, Yield: 88%; m. p. 79-80. IR spectrum, (KBr, ύ=$cm^{-1}$), N-$H_2$: 4433,3400, C-H arom.: 3020, C-H aliph.: 2866, C-Cl: 773. $^1$H NMR (400 MHz, DMSO) δ 7.06 (s, 1H, imidazole), 4.74 (s, 2H, $NH_2$), 4.67 (t, *J* = 5.9 Hz, 2H), 4.01 (t, *J* = 5.9 Hz, 2H), 2.53 (s, 3H). $^{13}$C NMR (101 MHz, DMSO) δ 149.17 (C-$NH_2$), 142.50, 115.99, 52.87, 48.26, 14.19(C$\underline{H}_3$). Anal. Calcd. For $C_6H_{10}ClN_3$ (159.62): C, 45.15; H, 6.32; Cl, 22.21; N, 26.33, Found C, 45.18; H, 6.34; Cl, 22.25; N, 26.39. LCMS: (ESI$^-$-MS, m/z) Calcd. for $C_6H_{10}ClN_3$ $(M-H)^-$: 159.62, Found: 158.69.

**General method for the synthesis of Schiff base compounds 3-6**

Dissolve (0.002 mol) of reduced compounds 1,2 in 25 ml of ethanol and add a (0.002 mol) solution of (p-nitro or p-chloro)-benzaldehyde with 3-4 drops of glacial acetic acid in 10 ml of ethanol. Heat the mixture in a reflux for 5-8 hours. The completion of the reaction was confirmed by TLC. The resulting mixture was left in a refrigerator, a precipitate formed, filtered, dried, and recrystallized in ethanol. The physical characteristics of Schiff bases-metronidazole 3-6 are itemized in Table 1.

**Table 1. The Physical Characteristics of Schiff Bases-Metronidazole 3-6**

| Compound No. | Chemical Structure | Mol. Wt. g/mol | Color | m.p°C | Yield |
|---|---|---|---|---|---|
| **3** | 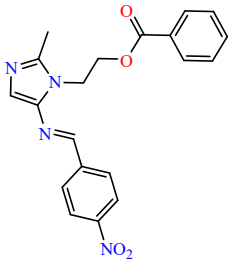 | 378.39 | Yellow | 148-150 | 77% |
| **4** | 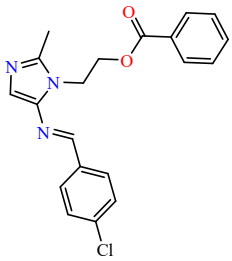 | 367.83 | Yellow | 129-130 | 74% |
| **5** | 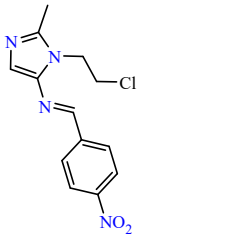 | 292.72 | Yellow | 133-134 | 72% |
| **6** | 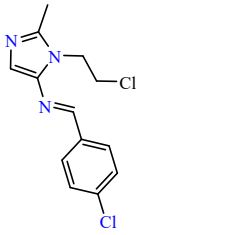 | 282.17 | Yellow | 123-125 | 70% |

**(E)-2-(2-methyl-5-((4-nitrobenzylidene) amino)-1H-imidazol-1-yl) ethyl benzoate—3**

Pale Yellow powder, Yield: 77%; m. p. 148-150. IR spectrum, (KBr, ύ=cm$^{-1}$), C-H arom.: 3058, C-H aliph.: 2993, C=O: 1726, $NO_2$ group: 1541,1375. $^1$H NMR (400 MHz, DMSO-d6) δ 9.09 (s, 1H,CH=N), 8.41 (d, J = 8.6 Hz, 2H), 8.16 (d, *J* = 8.6 Hz, 2H), 8.01 (d, *J* = 7.2 Hz, 1H), 7.76 (s, 1H), 7.66 (t, J = 7.6 Hz, 2H), 7.51 (t, *J* = 6.6 Hz ,2H), 4.61 (t, *J* = 19.3 Hz, 2H,O-$CH_2$), 4.39 (t, *J* = 10.6 Hz, 2H,N-$CH_2$), 2.47 (s, 3H).$^{13}$C NMR (101 MHz, DMSO) δ 168.81(C=O), 159.51(C-$NO_2$), 147.13, 146.62, 145.60, 145.48, 131.55, 131.09, 128.96, 128.80, 127.97, 127.82, 127.51, 127.40, 125.93, 124.10, 63.89, 46.42, 15.42. Anal. Calcd. For $C_{20}H_{18}N_4O_4$ (378.39): C, 63.49; H, 4.80; N, 14.81; O, 16.91, Found C, 63.51; H, 4.84; N, 14.85; O, 16.95. LCMS: (ESI$^-$-MS, m/z) Calcd. for $C_{20}H_{18}N_4O_4$ $(M-H)^-$: 378.39, Found: 377.41.

**(E)-2-(5-((4-chlorobenzylidene) amino)-2-methyl-1H-imidazol-1-yl) ethyl benzoate—4**

Pale Yellow powder, Yield: 74%; m. p. 129-130. IR spectrum, (KBr, ύ=cm$^{-1}$), C-H arom.: 3039, C-H aliph.: 2993, C=O: 1706, C-Cl: 773. $^{1}$H NMR (400 MHz, DMSO) δ 8.90 (s, 1H,C<u>H</u>=N), 8.01 (d, *J* = 7.4 Hz, 2H), 7.86 (s, 1H), 7.74 (q, *J* = 7.9 Hz, 2H), 7.64 – 7.50 (m, 3H), 7.50 – 7.41 (m, 2H), 7.23 (s, 1H), 4.60 – 4.43 (m, 2H, $CH_2$-O), 4.35 (d, *J* = 18.6 Hz, 2H, C<u>H</u>$_2$-N), 2.42 (s, 3H,$CH_3$). $^{13}$C NMR (101 MHz, DMSO) δ 165.61(<u>C</u>=O), 158.80, 148.44, 146.42, 145.84, 138.41, 132.97, 132.97, 130.82, 130.57, 129.62, 129.45, 128.86, 126.36, 125.22, 58.48, 47.80, 15.47 (<u>C</u>H$_3$). Anal. Calcd. For $C_{20}H_{18}ClN_3O_2$ (367.83): C, 65.31; H, 4.93; Cl, 9.64; N, 11.42; O, 8.70, Found C, 65.34; H, 4.96; Cl, 9.69; N, 11.45; O, 8.74. LCMS: (ESI$^-$-MS, m/z) Calcd. for $C_{20}H_{18}N_4O_4$ (M-H)$^-$: 367.83, Found: 366.77.

**(E)-N-(1-(2-chloroethyl)-2-methyl-1H-imidazol-5-yl)-1-(4-nitrophenyl) methanimine—5**

Dark Yellow powder, Yield: 72%; m. p. 133-134. IR spectrum, (KBr, ύ=cm$^{-1}$), C-H arom.: 3026, C-H aliph.: 2974, $NO_2$ group: 1533,1375, C-Cl: 778. $^{1}$H NMR (400 MHz, DMSO) δ 9.09 (s, 1H, CH=N), 8.42 (d, *J* = 8.7 Hz, 2H), 8.17 (d, *J* = 8.7 Hz, 2H), 7.10 (s, 1H), 4.41 (t, *J* = 7.2 Hz, 2H), 3.43 (t, *J* = 7.0 Hz, 2H), 2.51 (s, 3H). $^{13}$C NMR (101 MHz, DMSO) δ 159.60 (<u>C</u>H=N), 151.58(<u>C</u>-$NO_2$), 149.26, 141.21, 136.54, 127.54, 127.35, 125.69, 125.50, 122.56, 50.82, 44.11, 13.16(<u>C</u>H$_3$). Anal. Calcd. For $C_{13}H_{13}ClN_4O_2$ (292.72): C, 53.34; H, 4.48; Cl, 12.11; N, 19.14; O, 10.93, Found C, 53.39; H, 4.50; Cl, 12.19; N, 19.18; O, 10.99. LCMS: (ESI$^-$-MS, m/z) Calcd. for $C_{13}H_{13}ClN_4O_2$ (M-H)$^-$: 292.72, Found: 291.67.

**(E)-N-(1-(2-chloroethyl)-2-methyl-1H-imidazol-5-yl)-1-(4-chlorophenyl) methanimine—6**

Dark Yellow powder, Yield: 70%; m. p. 123-125. IR spectrum, (KBr, ύ=cm$^{-1}$), C-H arom.: 3062, C-H aliph.: 2974, C-Cl: 810. $^{1}$H NMR (500 MHz, DMSO-$d_6$) δ 8.90 (s, 1H, CH=N), 7.72 – 7.68 (m, 4H), 6.94 (s, 1H, imidazole), 4.38 (t, *J* = 1.0 Hz, 2H), 4.01(t, *J* = 1.0 Hz, 2H), 2.47 (s, 3H). $^{13}$C NMR (101 MHz, DMSO) δ 157.83(<u>C</u>H=N), 146.60, 140.16, 133.53, 131.32, 128.89, 128.69, 123.19, 47.29, 44.49, 15.19(<u>C</u>H$_3$). Anal. Calcd. For $C_{13}H_{13}Cl_2N_3$ (282.17): C, 55.34; H, 4.64; Cl, 25.13; N, 14.89, Found C, 55.39; H, 4.68; Cl, 25.16; N, 14.91. LCMS: (ESI$^-$-MS, m/z) Calcd. for $C_{13}H_{13}Cl_2N_3$ (M-H)$^-$: 282.17, Found: 281.23. the selected spectra for $^{1}$H NMR and $^{13}$C NMR of compound in current study (Met.b; and Met.Cl compounds are shown in Figures 1 and 2, respectively).

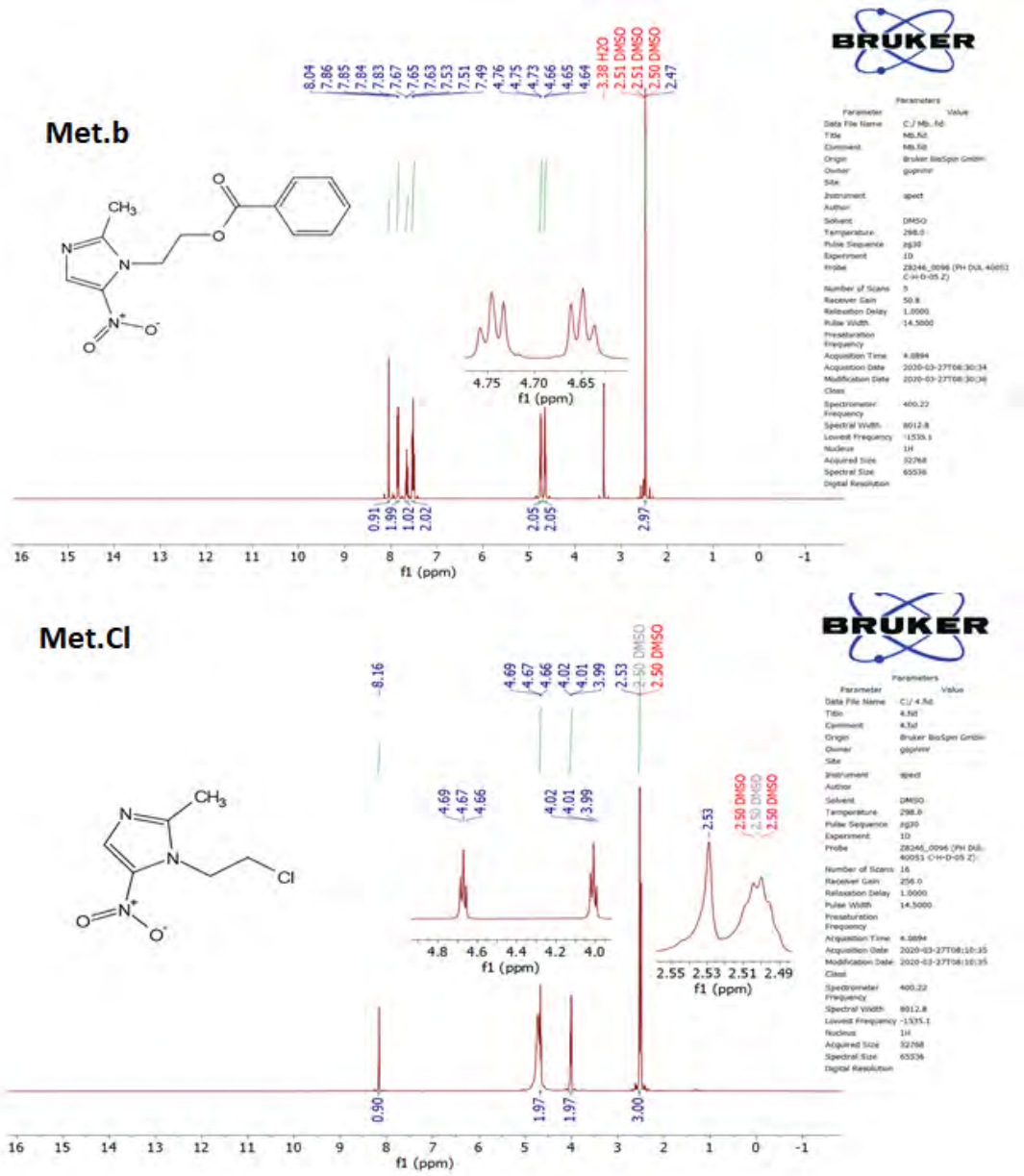


**Figure 1. $^{1}$HNMR Spectra for Met.b**: 2-(2-methyl-5-nitro-1H-imidazol-1-yl) ethyl benzoate; **Met.Cl**: 1-(2-chloroethyl)-2-methyl-5-nitro-1H-imidazole

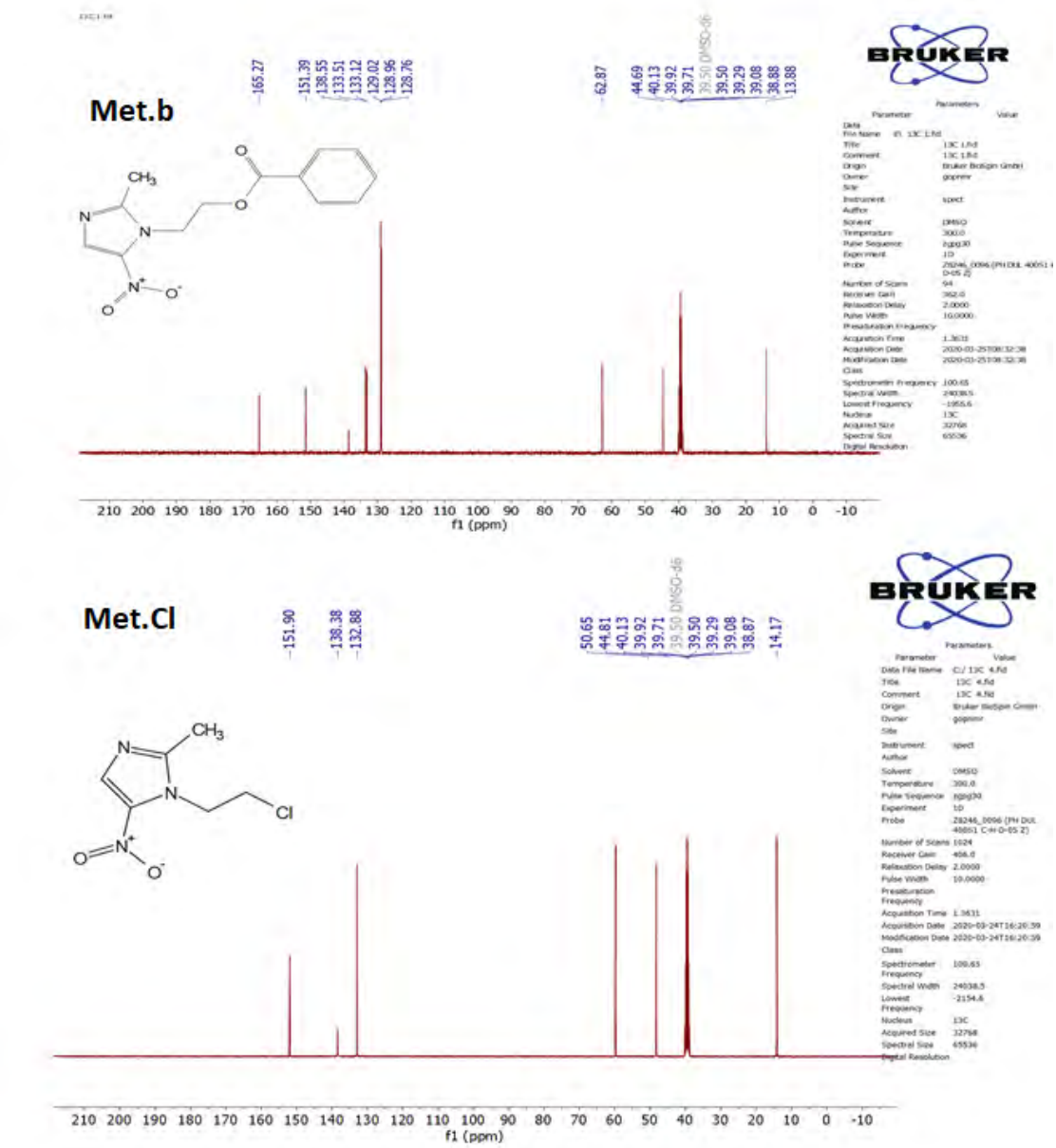


**Figure 2. $^{13}$CNMR Spectra for Met.b**: 2-(2-methyl-5-nitro-1H-imidazol-1-yl) ethyl benzoate; **Met.Cl**: 1-(2-chloroethyl)-2-methyl-5-nitro-1H-imidazole

## Biological Evaluation

The antibacterial activity was carried out in the laboratories of the Department of Biology/College of Education/University of Samarra. *Pseudomonas aeruginosa*, a gram-negative bacterium, and *Staphylococcus aureus*, a gram-positive bacterium, were isolated from patients at Samarra General Hospital and diagnosed using Vitck 2. The agar diffusion method was used by Wells etching on Muller-Hinton Agar medium. Cork borers were drilled with equal dimensions to prevent overlapping of inhibition diameters and with a diameter of 6 mm, to contain 0.5 ml of compound solutions for each hole after spreading 1.0 ml of bacterial suspension on the medium to

test the sensitivity of bacteria to the prepared compounds at concentrations of 25, 50, and 100 mg/ml using DMSO as a solvent. Then, the plates were incubated at 37°C for 24 hours, and the results were read by measuring the diameter of the inhibition zone [20,21]. The images of the bacterial plates are shown in Figures 3 and 4.

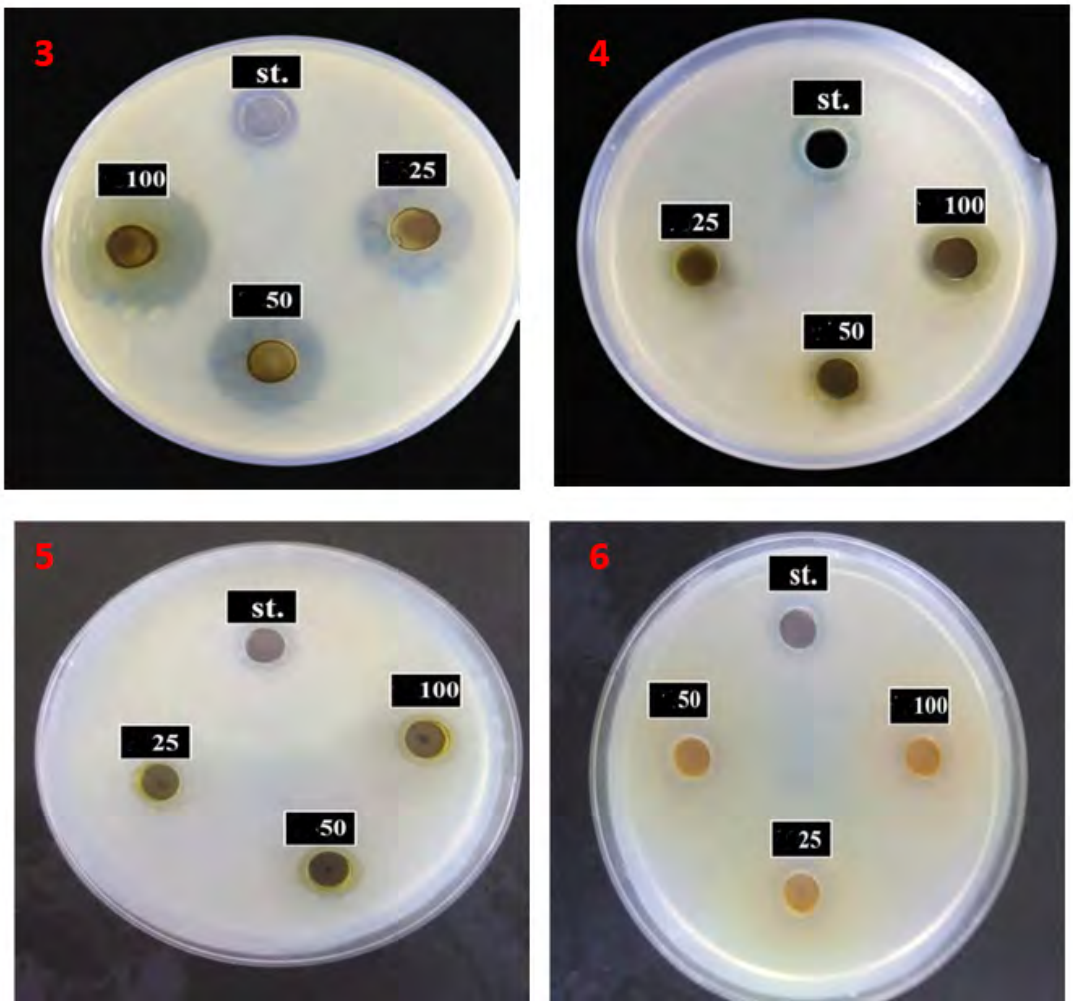


**Figure 3. Inhibitory Activity of the Prepared Compounds against *Pseudomonas aeruginosa*** (**3**: (E)-2-(2-methyl-5-((4-nitrobenzylidene) amino)-1H-imidazol-1-yl) ethyl benzoate; **4**: (E)-2-(5-((4-chlorobenzylidene) amino)-2-methyl-1H-imidazol-1-yl) ethyl benzoate; **5**: (E)-N-(1-(2-chloroethyl)-2-methyl-1H-imidazol-5-yl)-1-(4-nitrophenyl) methanimine; **6**: (E)-N-(1-(2-chloroethyl)-2-methyl-1H-imidazol-5-yl)-1-(4-chlorophenyl) methanimine)

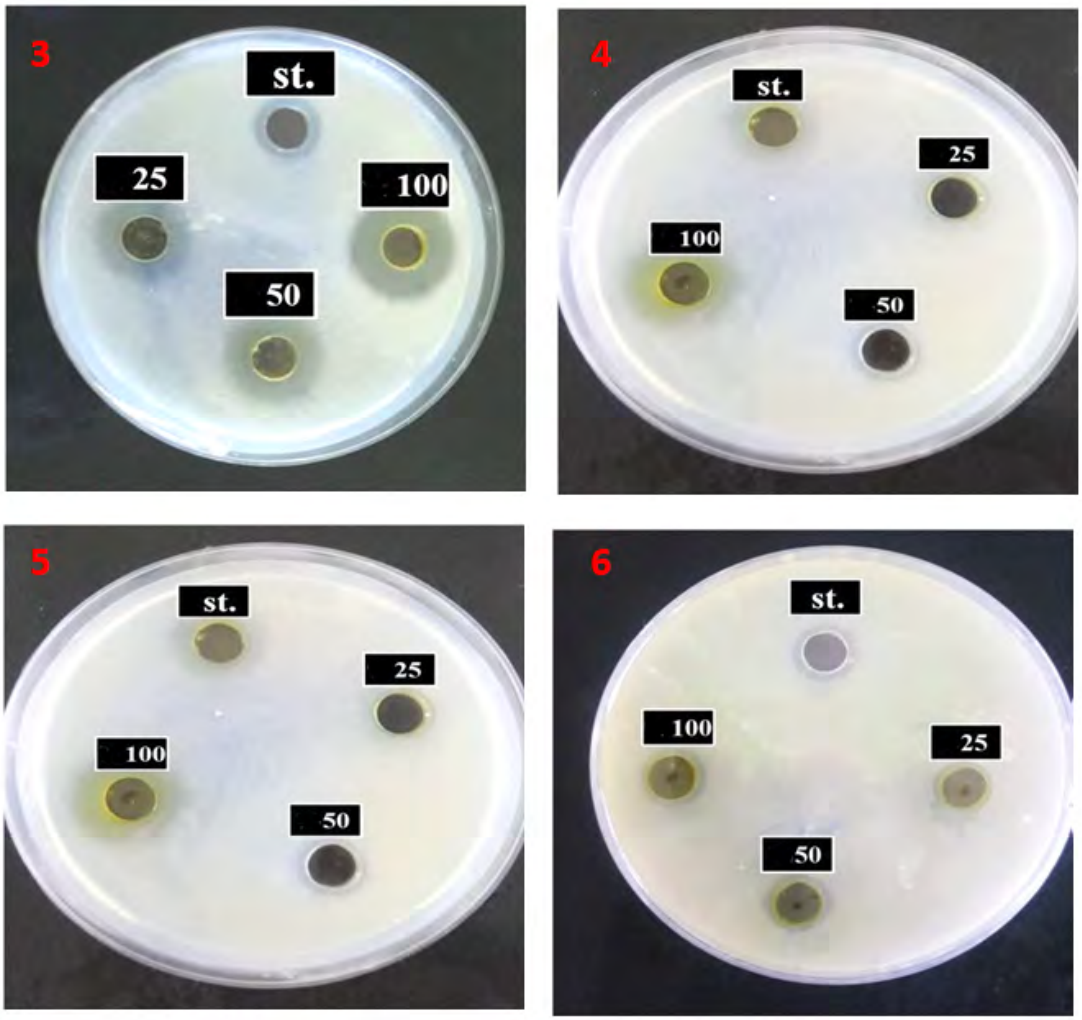


**Figure 4. Inhibitory Activity of the Prepared Compounds Against *Staphylococcus aureus*** (**3***:* (E)-2-(2-methyl-5-((4-nitrobenzylidene) amino)-1H-imidazol-1-yl) ethyl benzoate; **4**: (E)-2-(5-((4-chlorobenzylidene) amino)-2-methyl-1H-imidazol-1-yl) ethyl benzoate; **5**: (E)-N-(1-(2-chloroethyl)-2-methyl-1H-imidazol-5-yl)-1-(4-nitrophenyl) methanimine; **6**: (E)-N-(1-(2-chloroethyl)-2-methyl-1H-imidazol-5-yl)-1-(4-chlorophenyl) methanimine)

## *In silico* Studies

### Ligand preparation

The series of synthesis metronidazole derivatives. The ligands were first sketched using ChemDraw 2020. Their two-dimensional structures were then converted into three-dimensional structures using Chem3D. This allowed molecular viewing and structural manipulation. The 3-D structures were kept in the mol2 file format and then were converted to .pdb format with Open Babel. This was done to ensure that the structures can be used by AutoDock.

In turn, prior to docking, all hydrogen atoms were introduced into the structures with the

help of the “Add Hydrogens” option in AutoDock Tools (ADT). In this way, proper valence and adequate protonation levels were achieved. Next, each compound was protonated via the “Protonate 3D” tool in Discovery Studio 4.5. In this way, the ionization levels were adjusted according to the physiological conditions, namely, pH 7.4. Moreover, this step made sure that the molecules had realistic charge values. Thus, the structures were once again saved in the .pdb format. Then, the ligands were processsed with AutoDock Tools, MGLTools, v1.5.7. In this step, Gasteiger partial charges were assigned to all atoms.

Moreover, non-polar hydrogens were combined to make the calculations of the molecule more convenient. The definition of flexible and rotatable bonds with ADT helped the docking software to study many different configurations of the ligand while docking. The last thing to do was to save the structure of the ligands in the .pdbqt format, which is needed for docking in AutoDock Vina [22].

**Receptor preparation**

We retrieved the crystal structures of target proteins from RCSB-PDB. Specifically, we selected bacterial *Pseudomonas aeruginosa* with target LpxC enzyme (PDB ID: 3U1Y) and bacterial gram-positive *Staphylococcus aureus* complex structure of Moxifloxacin with *S. aureus* DNA gyrase and DNA (PDB ID;5CDQ) as receptors models for docking experiments. We chose these structures for their high-resolution data and co-crystallized ligands, which allow us to determine active sites with greater precision.

The downloaded PDB file was prepared for docking using Discovery Studio Visualizer 4.5 software by deleting any molecule of water, ion, or any other heteroatom that does not bind to the protein. The cocrystalized ligands (native cocrystals of 3U1Y, and cocrystals (Moxifloxacin) of 5CDQ) were kept temporarily to identify the active site, but later on deleted before performing docking studies.

Further modification was done on receptors through AutoDock Tools (ADT) and MGLTools Version 1.5.7. Polar hydrogens were introduced to properly simulate hydrogen bonding. On the other hand, nonpolar hydrogens were combined to decrease the number of atoms used in computations. Kollman united atom charges were introduced in all protein atoms. These charges are needed in docking because they allow for electrostatic calculations. Active sites were identified based on the crystal structure of coexisting ligands.

All the receptors were saved in .pdbqt format, which is mandatory while carrying out docking in AutoDock Vina. This technique improved the models of receptors for LpxC enzyme (PDB ID: 3U1Y), and bacteria gram-positive (PDB ID: 5CDQ) [23].

**Docking Method**

Molecular docking studies were carried out using AutoDock Vina, which was installed on a computer running the Windows 10 operating system, comprising 32 cores. This

analysis was aimed at predicting the most favorable binding mode as well as binding energy for the ligand-target interaction, especially focusing on grid box parameters. The parameters were defined using AutoDock Tools (ADT). When setting the grid box location, the crystallographic binding site of the ligands was taken into account. Since proper conformational sampling was to be ensured, the size of the grid box was marginally adjusted. This allowed the flexible monomeric units of synthesized ligands and their free side chains sufficient rotational and translational freedom during the docking process [24].

The coordinates of the binding site for the gram-positive target protein (PDB ID: 5CDQ) were taken from the X-ray crystal structure. Here, the grid box with dimensions of 64 × 64 × 64 grid points at an interval of 0.375 Å with coordinates x = 41.504, y = -52.516, and z = 65.034 was generated, thus leading to 274,625 grid points per grid map.

For LpxC (PDB ID: 3U1Y), the docking grid box was generated around the co-crystallized ligand binding site. The grid dimensions were 60 × 54 × 70 points with a grid spacing of 0.375 Å and center coordinates of x = 16.508, y = 2.197, and z = 24.593. Docking calculations were then performed using AutoDock Vina, and ten binding poses were generated for each ligand. The best binding pose of all generated binding poses was selected based on its highest binding affinity value (kcal/mol). Default values for scoring and optimization were maintained.

The analysis and depiction of the ligand-receptor binding interactions, which include hydrogen bonding, hydrophobic interactions, and pi-pi stacking, were performed using AutoDock Tools and Discovery Studio 4.5 [25].

**Visualization and interpretation of docking results**

Among the AutoDock Vina output, the conformations of the ligands with the lowest binding energies (kcal/mol) were selected. In order to study and visualize the specific binding interactions of the ligands with the receptors at their respective binding sites, Discovery Studio Visualizer (DSV; 64-bit Windows 10) was used.

DSV analysis yielded various types of molecular interactions, for example hydrogen bond formation, hydrophobic effect, and metal binding, among others. Through this analysis, an understanding was gained about the nature of the ligand-receptor binding and the critical residues involved in such interactions. Interaction diagrams were derived from the 2D DSVs and 3D binding visualizations. They were originally simple images but were subsequently saved in .tif format.

**Validation of results**

The validity of the docking technique was evaluated by carrying out redocking experiments utilizing the ligands found in the crystal structure of the target proteins.

In the case of gram-positive target (5CDQ), the co-crystallized ligand, namely, Moxifloxacin was stripped off, and it was then docked again back into the protein's active site using the exact docking procedure that was applied on the metronidazole derivatives. DSV analysis was employed to precisely determine the ligand-receptor interaction sites, in addition to identifying all other types of interactions that may take place between the molecules, such as hydrogen bonding and hydrophobic interaction. The docking of metronidazole derivatives was validated by comparing their predicted binding mode with that of the reference ligand.

The docked complex formed by the gram-negative drug target-inhibitor (PDB ID: 3U1Y) was first removed from its bacterial LpxC protein target, after which it was subsequently re-docked back into its active site region in order to reproduce the binding mode observed experimentally. DSV technique was utilized in mapping the interaction of the inhibitor molecule with the active site residues. These data served as controls for the validation of the docking process.

This docking method employed in this experiment to the two sets of target proteins provided a good benchmark for the targets. In this way, an accurate prediction of the binding activity of the ligand under consideration was assured. This helped to ensure the accuracy of the docking results of the synthesized ligands [26,27].

## 3. Results and Discussion

### Chemistry

The Schiff-metronidazole target bases were prepared by modifying the nitro and hydroxyl groups in metronidazole by converting it to the corresponding ester and chloro derivative, then reducing the nitro group using $Na_2S_2O_4$ as a mild reducing agent, as following the previous method research [22], to prepare an amine group to enter the Schiff reaction with a 4-nitro or 4-chlorobenzaldehyde, where the condensation reaction took place in an acidic medium of acetic acid and by refluxed to obtain Schiff bases 3-6, as shown in Scheme 1.

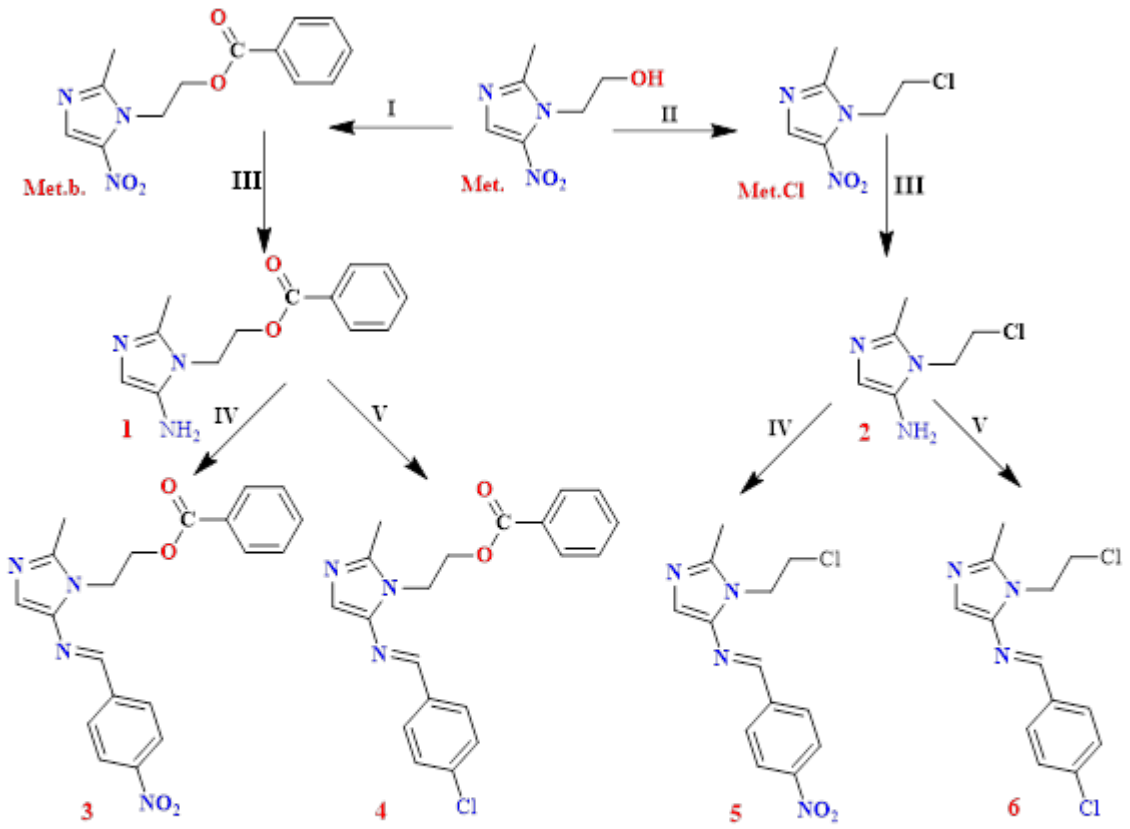


I = benzoyl chloride,pyridine, II = $SOCl_2$,diethyl ether,room temp.

III =reduced agent : $Na_2S_2O_4$

IV = p-Nitobenzaldehyde,$CH_3COOH$,EtOH,Refluxe 4-5 h.

V = p-Chlorobenzaldehyde,$CH_3COOH$,EtOH,Refluxe 4-5 h.

**Scheme 1. Synthesis of the Schiff Bases-Metronidazole Target Compounds 3-6**

This reaction is carried out via the common mechanism for preparing Schiff bases, where first, the nucleophilic addition reaction of the amine to the carbonyl group of the aldehyde takes place after protonation with the acid as a catalyst for the carbonyl to increase its electrophilicity, and second, the elimination step by removing the water molecule and removing the acid proton to obtain the target Schiff bases 3-6, as shown in Scheme 2.

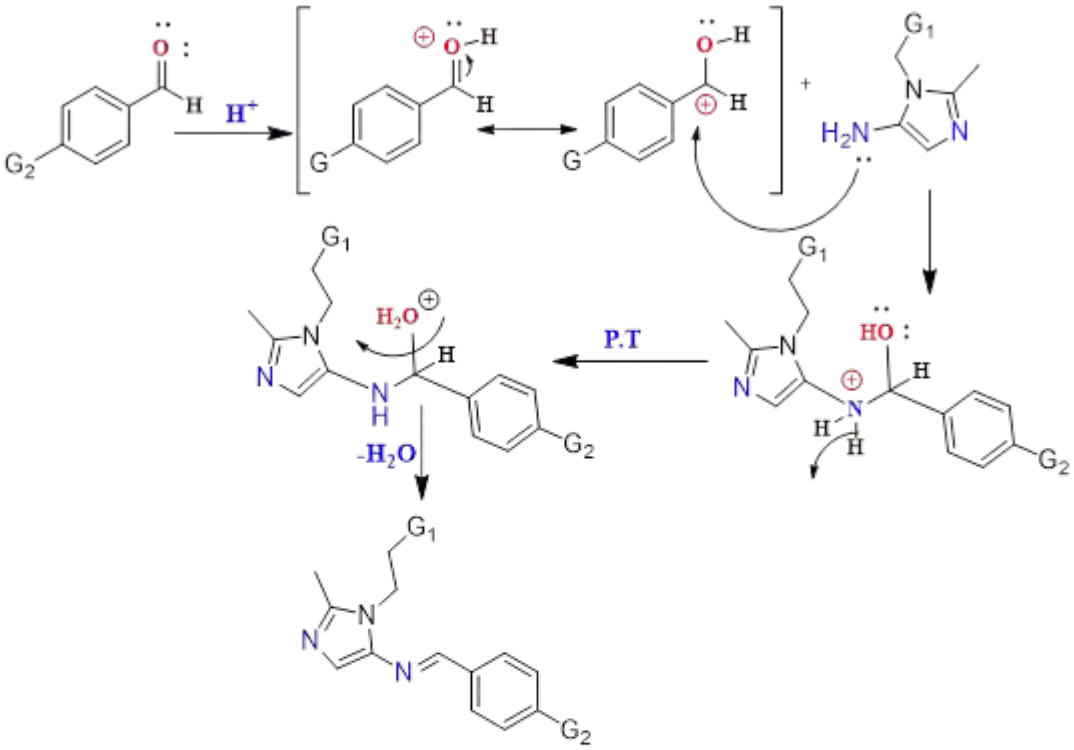


Metronidazole-Schiff bases 3-6

| Comp. No. | 3 | 4 | 5 | 6 |
|---|---|---|---|---|
| G1 | 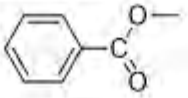 | 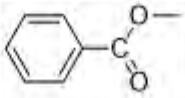 | -Cl | -Cl |
| G2 | $-NO_2$ | -Cl | $-NO_2$ | -Cl |

**Scheme 2. Mechanism Synthesis of the Schiff-Metronidazole 3-6**

FTIR spectroscopy was used to characterize the precursor 1,2 the reduced Metronidazole. The spectra showed: disappearance of the bands of the $–NO_2$ group at about (1541-1361) $cm^{-1}$, two absorption bands appeared due to the asymmetric and symmetric stretching of $-NH_2$ at about 3452-3363 $cm^{-1}$, and this confirms reduction of the Nitro group. Also, the $^{1}H$ & $^{13}C$-NMR spectra confirmed the appearance of a proton signal for the amine group $NH_2$ at 7.55,4.74 ppm and a signal at 153.67,149.17 ppm for the carbon attached to it (Figure 5).

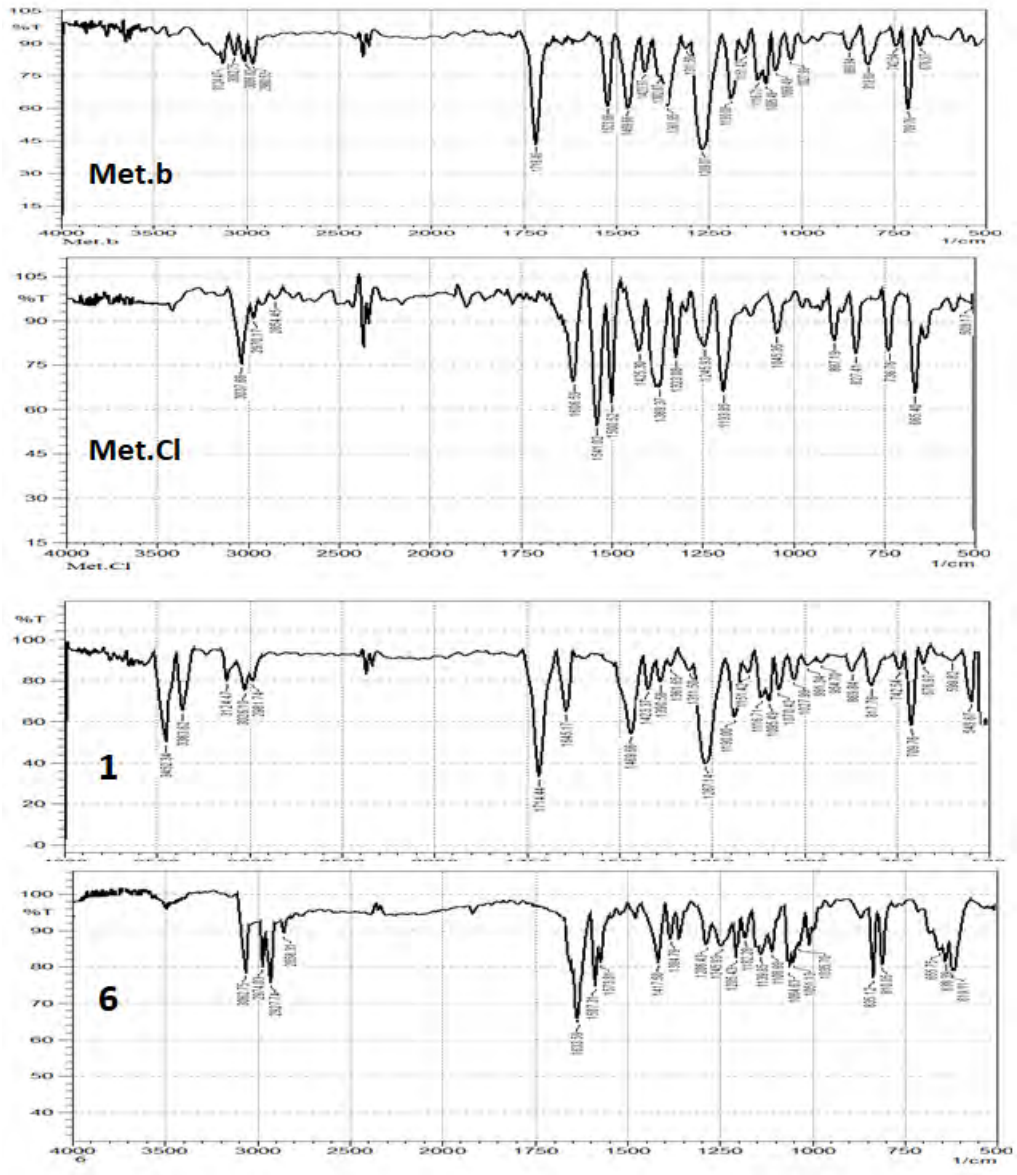


**Figure 5. FT-IR Spectra for Met.b:** 2-(2-methyl-5-nitro-1H-imidazol-1-yl) ethyl benzoate; **Met.Cl**: 1-(2-chloroethyl)-2-methyl-5-nitro-1H-imidazole; **1**: 2-(5-amino-2-methyl-1H-imidazol-1-yl) ethyl benzoate; **6**) (E)-N-(1-(2-chloroethyl)-2-methyl-1H-imidazol-5-yl)-1-(4-chlorophenyl) methanimine

The structures of Schiff bases-metronidazole derivatives were identified and confirmed by FTIR spectroscopy. The spectra showed the disappearance of the two amine stretch bands and the appearance of a medium-intensity stretch band of the azomethine bond, which overlaps with the aromatic C=C stretch bands of the compounds at 1500-1600 $cm^{-1}$. As for the $^{1}H$ & $^{13}C$-NMR spectra, the azomethine proton signal appeared at 8.90, 9.09 ppm, in addition to the appearance of the methyl signal at 2.42-2.51 ppm, the triple signals duo to -$CH_2$-$CH_2$- at about 3.43-4.61 ppm, and the aromatic protons appeared in the range of 6.94-8.42 ppm, while the carbonyl carbon of the corresponding 3,4 ester derivative appeared at 168.81, 165.61 ppm.

## Biological Activity

To explore the antibacterial activity of the newly synthesized homologues, Schiff bases 3-6 were tested against *Pseudomonas aeruginosa*, a gram-negative bacterium, and *Staphylococcus aureus*, a gram-positive bacterium. These bacteria were carefully selected because they cause common and serious human diseases, exhibit resistance to many known antibiotics, are easy to culture, and exhibit antibacterial properties.

Hybrid metronidazole Schiff bases 3-6 were selected to test their antibacterial activity against *Pseudomonas aeruginosa* and *Staphylococcus aureus*. The tested compounds showed good activity against both bacterial species compared to metronidazole and metronidazole benzoate, as measured by zones of inhibition. Derivatives 3 and 4 showed the best inhibition against *Pseudomonas aeruginosa* at 100 mg/ml (21 and 20 mm), respectively, outperforming metronidazole (15 mm). Furthermore, compounds 3, 4, and 5 showed good activity against *Staphylococcus aureus*: (25, 23, and 22 mm), respectively, at 100 mg/ml compared to the reference antibiotic, metronidazole. Conversely, it was found that compound 3 achieved the highest inhibition even at a concentration of 25 mg/ml. This relates to the structure-activity relationship, as compound 3 contains a nitro group at the para position in the phenyl ring, which enhances the electronic properties for binding to the bacterial protein.

Figures 6 and 7 and the attached images of the plates illustrate the bacterial activity of both types.

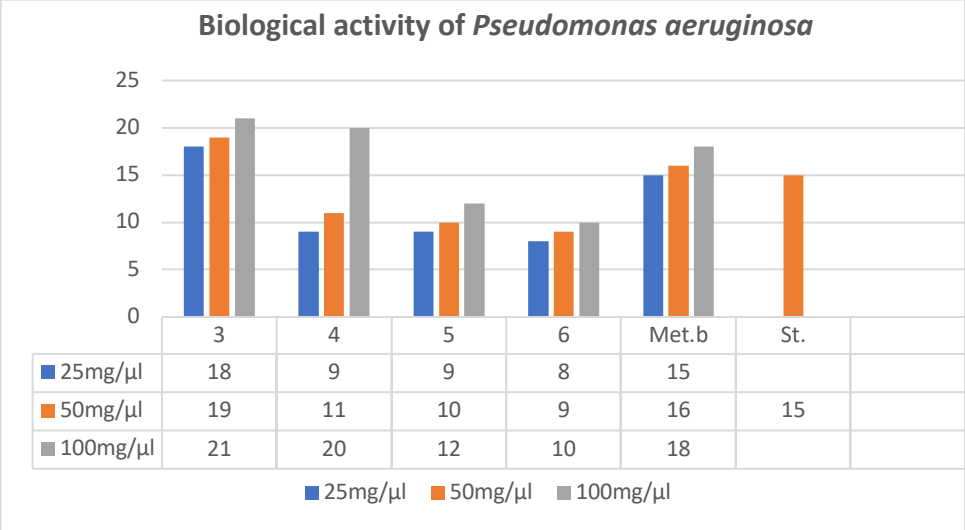


**Figure 6. Inhibitory Activity of the Prepared Compounds Against *Pseudomonas aeruginosa***

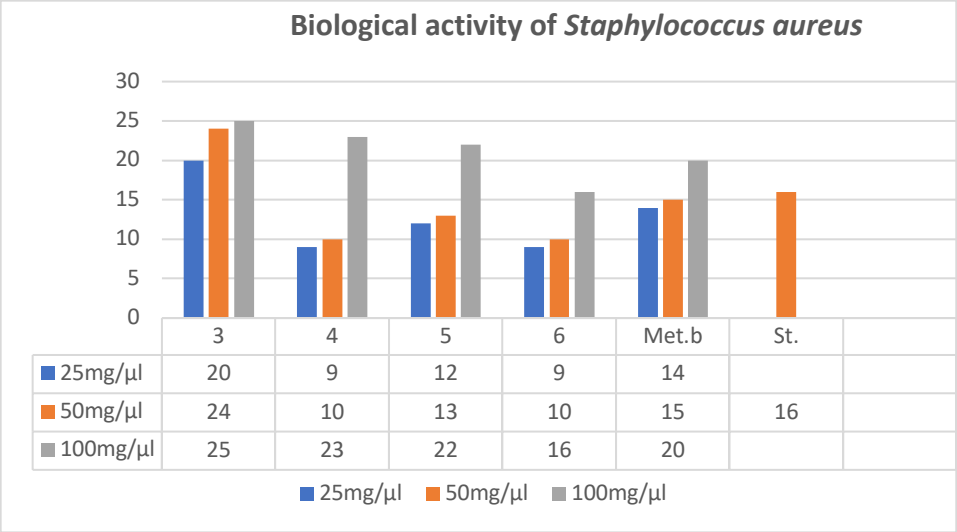


**Figure 7. Inhibitory Activity of the Prepared Compounds Against *Staphylococcus aureus***

## Molecular Docking

Molecular docking studies of synthesized metronidazole derivatives compounds against various bacterial targets indicated promising interactions, as indicated by the docking scores, are shown in Table 2.

**Table 2. The Physical Characteristics of Schiff Bases-Metronidazole 3-6**

| Name | 2D Structure | Dock score interaction energy for bacteria (gram-positive) kcal/mol pdb code 5CDQ | Dock score interaction energy for bacteria (gram-negative) kcal/mol pdb code 3U1Y |
|---|---|---|---|
| Positive control (co-crystal ligand Moxifloxacin) (pdb:5CDQ ) | 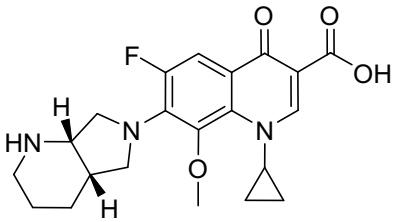 | -10.58 | / |
| Positive control (co-crystal ligand (pdb:3U1Y) | 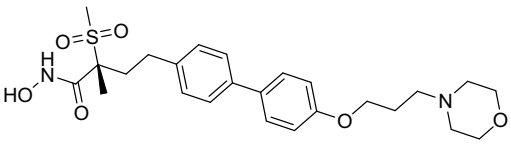 | / | -7.48 |

| | | | |
|---|---|---|---|
| **3** | 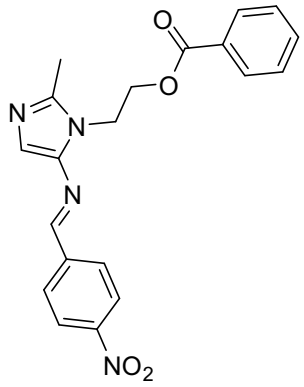 | -9.15 | -7.36 |
| **4** | 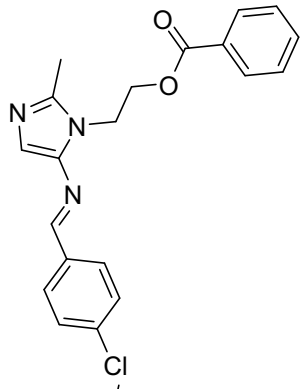 | -8.13 | -7.36 |
| **5** | 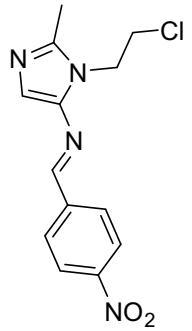 | -7.93 | -6.25 |
| **6** | 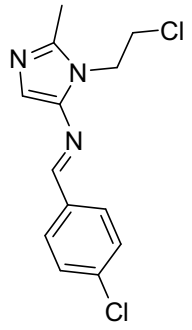 | -6.97 | -5.58 |
| **Met.** | 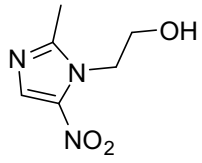 | -6.15 | -5.01 |

| | | | |
|---|---|---|---|
| **Met.Cl** | 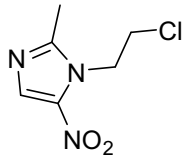 | -5.81 | -4.86 |
| **Met.b** | 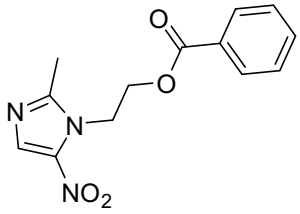 | -7.09 | -6.67 |

For compound 3, the gram-positive bacterial target with a PDB ID of 5CDQ yielded a docking score of -9.15 kcal/mol, indicating strong interactions. Attractive charge, p-anion bonds were observed with amino acids ARG A:122, PTR A:123, and GLU D:477, along with extended bonding with nucleotide DT E:8. Hydrophobic interactions (p-p stacked, p-Alkyl) with nucleotides, including DG E:2009, DA F:2013, and DC F:2012, help stabilize the complex and increase its affinity for the active site, as shown in Figure 8.

A

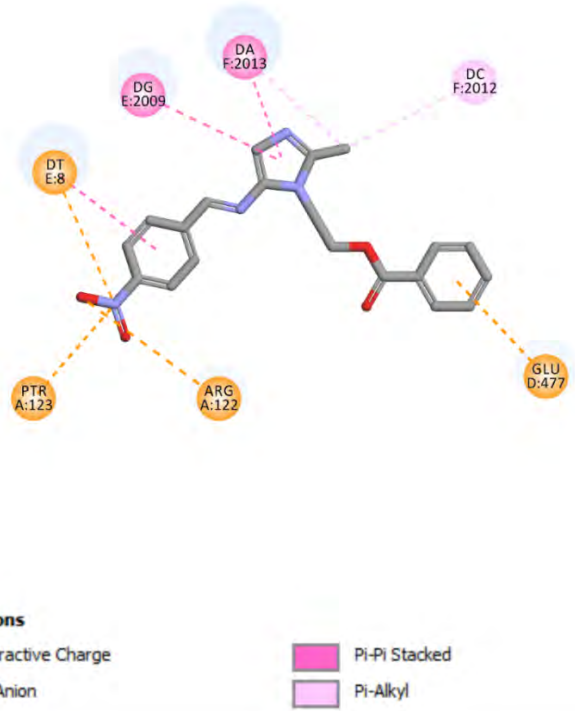

B

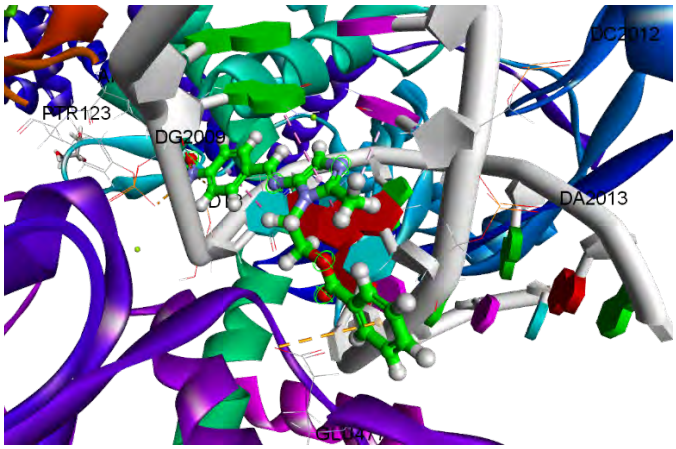


**Figure 8. (A) 2D Interactions of Compound 3 Inside 5CDQ Target, (B) 3D Interactions of Compound 3 Inside 5CDQ Target**

For the gram-negative bacterial target (PDB ID: 3U1Y), compound 3 showed a favorable docking score of -7.36 kcal/mol, indicating good binding affinity toward the active site. Structural analysis revealed that the benzene–nitro moiety formed conventional hydrogen bonds with THR B:190 and PHE B:191**.** Additionally, the ligand exhibited π–cation**,** π–anion, and electrostatic attractive interactions with ASP B:241, which collectively enhanced binding stability. Hydrogen bonding occurred between carbonyl group of ester bridge with LYS B:142. A metal-acceptor and attractive charge interaction with the catalytic $Zn^{2+}$ ion further stabilized the binding, further π- π stacked with PHE B:160 and additional hydrophobic interactions with amino acids, including THR B:60, THR B:61, ILE B:158, LYS B:261, HIS B:264 and ALA B:265, help stabilize the complex and increase its affinity for the active site, as shown in Figure 9.

A

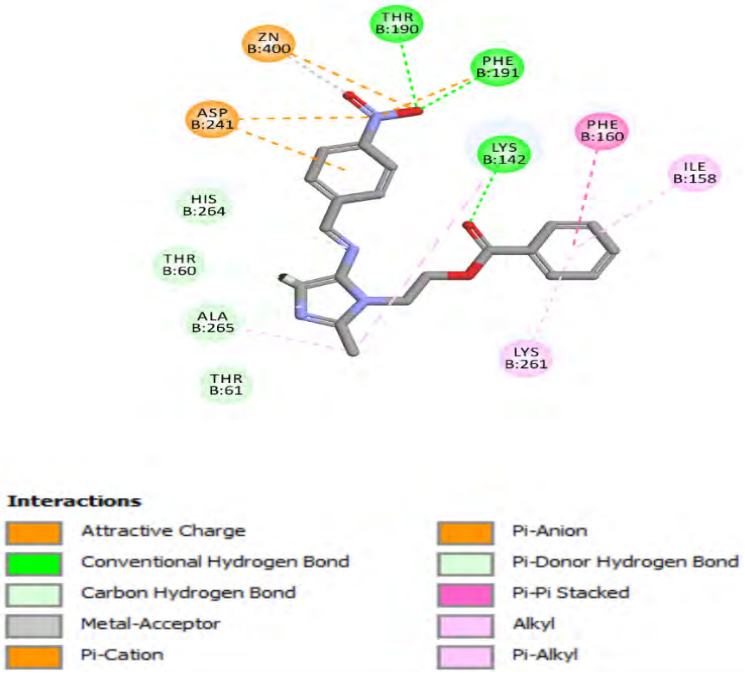

B

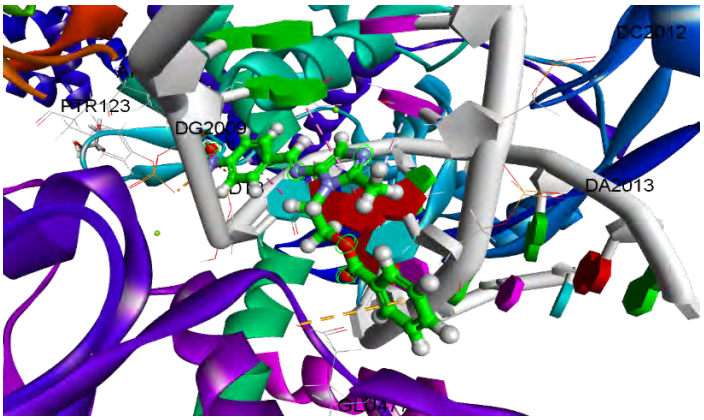


**Figure 9. (A) 2D Interactions of Compound 3 Inside 3U1Y Target, (B) 3D Interactions of Compound 3 Inside 3U1Y Target**

In the pose for compound 4, the gram-positive bacterial target showed a docking score of -8.13 kcal/mol against PDB ID 5CDQ, with important interactions involving hydrogen bonding with DA F:2013, as well as three π-cation bonds with nucleotides DT E:8, DG E:2009, DC F:2012. Also, it showed π-anion interaction with the amino acid GLU D:477. Furthermore, the complex is stabilized by hydrophobic interactions with DT E:8, DG E:2009, and DA F:2013, as illustrated in Figure 10.

A

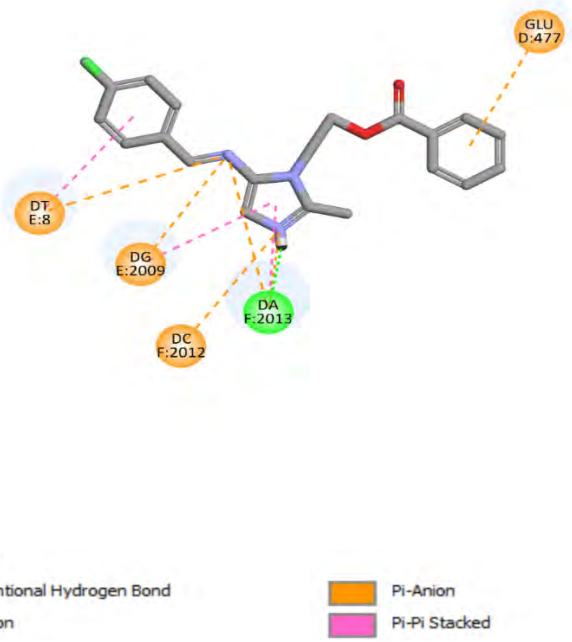

B

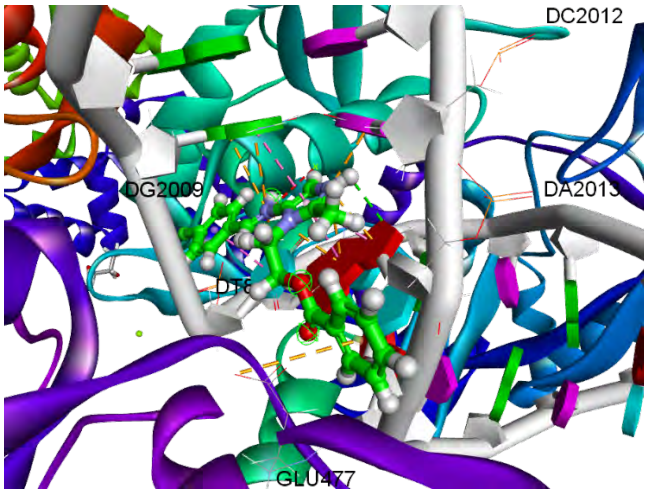


**Figure 10. (A) 2D Interactions of Compound 4 Inside 5CDQ Target, (B) 3D Interactions of Compound 4 Inside 5CDQ Target**

For the gram-positive bacterial target (PDB ID: 3U1Y), although no direct coordination with the $Zn^{2+}$ ion was detected, compound 4 demonstrated multiple stabilizing non-covalent interactions within the active site. The carbonyl and ester oxygen atoms formed hydrogen bonds with LYS B:142 and LYS B:238**,** respectively. The ionized pyrazole NH group established hydrogen bonding interactions with THR B:6 and THR B:61, while the imine nitrogen atom exhibited an attractive electrostatic interaction with ASP B:241. Additionally, the benzene ring participated in a π–anion interaction with ASP B:241, whereas π–π stacking interactions were observed between the aromatic rings of compound 4 and PHE B:160 and PHE B:191, contributing to the stabilization of the ligand–protein complex. Furthermore, hydrophobic interactions with amino acids, including ILE B:158, HIS B:237, LYS B:261, and ALA B:265, help stabilize the complex and increase its affinity for the active site, as shown in Figure 11.

A

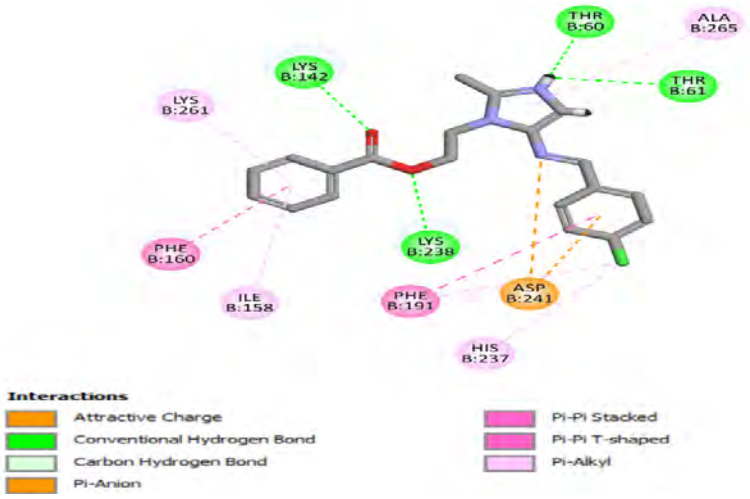

B

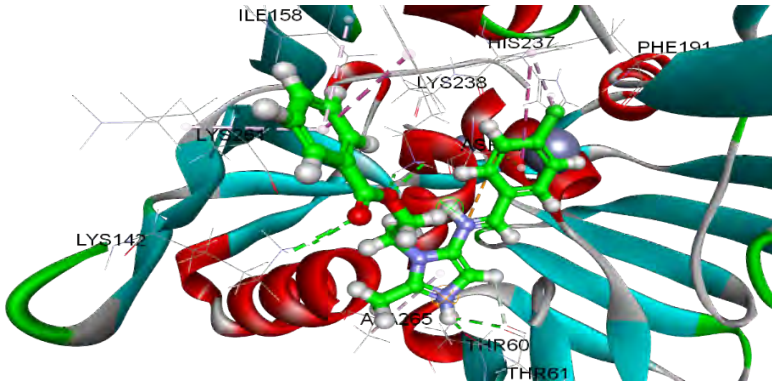


**Figure 11. (A) 2D Interactions of Compound 4 Inside 3U1Y Target, (B) 3D Interactions of Compound 4 Inside 3U1Y Target**

## 5. Conclusion

This research was designed to develop new antibacterial agents via Schiff bases from metronidazole, which showed a significantly more inhibitory effect than metronidazole against *Staphylococcus aureus* and *Pseudomonas aeruginosa*. Compound 3 gave the highest inhibition of both types of bacteria at a diameter of 21,25 mm, respectively, at a concentration of 100 mg/ml. Also, in the docked study, the compound 3 has the best binding site from metronidazole derivatives for both protein targets, where for bacteria *Staphylococcus aureus* (gram-positive), pdb code 5CDQ, and for bacteria *Pseudomonas aeruginosa* (gram-negative), pdb code 3U1Y.This is attributed to the presence of electron pairs of the nitrogen atom in azomethine, as well as the presence of the electron-withdrawing nitro group in the para position, which gives the compound high electronic properties due to resonance and conjugation, thus enhancing the binding to bacterial proteins. These conclusions afford an insight into the expansion and optimization of more effective antibacterial Schiff bases.

## 5. Disclosure of Interest

The authors declare that they have no known competing financial interests or personal relationships that could have appeared to influence the work reported in this paper.

## 6. Funding

The authors report that there is no funding associated with the work featured in this article.

## 7. References


1. Dini I. Mechanisms of bacterial resistance and innovative strategies to overcome antimicrobial resistance. *Antibiotics*, 2026, 15(3), 319. https://doi.org/10.3390/antibiotics15030319
2. Löfmark S, Edlund C, Nord CE. Metronidazole is still the drug of choice for treatment of anaerobic infections. *Clin. Infect. Dis.*, 2010, 50(Supplement_1), S16–S23.
3. Aachari A, Khamar M, Cherkaoui E, Bechar S. Synthesis, structural characterization, and antimicrobial evaluation of dimethyl methylene phosphate: An innovative phosphorylated compound with broad-spectrum potential. *Chemist*, 2025, 96(1).
4. Shahzad I, Alasmari MS, Zamir A, Rasool MF, Alqahtani F. Clinical pharmacokinetics of metronidazole: A systematic review and meta-analysis. *Antimicrob. Agents Chemother.*, 2025, 69(9), e01904-01924.
5. Ayinde O, Ross JD. The frequency and duration of side-effects associated with the use of oral metronidazole: A prospective study of VITA trial participants. *Int. J. STD AIDS*, 2023, 34(12), 897-902.
6. Ahmadi H, Heydari M, Abdouss M, Jamalpoor Z, Fathi-Karkan S, Rahdar A, Pandey S. Metronidazole delivery strategies: Optimizing cancer therapy through novel approaches for enhanced delivery, cytotoxicity, and side effect reduction. *Eur. J. Med. Chem. Rep.*, 2024, 12, 100202.
7. Khabnadideh S, Rezaei Z, Khalafi Nezhad A, Motazedian MH, Eskandari M. Synthesis of metronidazole derivatives as antigiardiasis agents. *Daru, J. Pharm. Sci.*, 2007, 15(1), 17-20.
8. Dhahir, AA, Hussein MS, Mohammed MO. Synthesis and antibacterial evaluation of new derivatives of metronidazole. *Int. J. Pharm. Res.*, 2020, 12, 1210-1220.
9. Mohammad HJ, Hussein MS. Synthesis of new scaffolds thiazolidine-4-one ring and characterization from derivatives of 1, 3-benzodioxole Schiff bases and its activity on antioxidant, molecular docking with PDE3A. *AIP Conf. Proc.*, 2024, 3219(1), 050003.
10. Wang SF, Yin Y, Qiao F, Wu X, Sha S, Zhang L, Zhu HL. Synthesis, molecular docking and biological evaluation of metronidazole derivatives containing piperazine skeleton as potential antibacterial agents. *Bioorg. Med. Chem.*, 2014, 22(8), 2409-2415.
11. Chen N, Yang L, Ding N, Li G, Cai J, An X, Wang, Z, Qin J, Niu Y. Recurrent neural network (RNN) model accelerates the development of antibacterial metronidazole derivatives. *RSC Adv.*, 2022, 12(35), 22893-22901.
12. Hassan KH, Al-Hussaniy HA, Ibraim Oraibi A, Bashar Al-Qazzan M, Zainee HY, Al-Jashamy K, Imad Hussein M. Thermodynamic and kinetic assessment of cobalt II adsorption using green synthesized NiO/γ-$Al_2O_3$ nanoparticles. *Salud, Ci. Tecnol. - Ser. Conf.*, 2025.
13. Noory MS, Hussein MS. Synthesis and characterization of 2-pyrone compounds derived from coumalic acid and evaluation of the antimicrobial activity of some of them. *AIP Conf. Proc.*, 2023, 2834(1), 030025.

14. Humeedi MD, Hussein MS. Synthesis new derivatives of quinoline and study the biological activity for some of them. *AIP Conf. Proc.*, 2022, 2450(1), 020019.
15. Kassan NE, Saadeh HA, Talib WH, Mahasneh AM, Kaur H, Goyal K, Sehgal R, Mubarak MS. Synthesis and biological activity of novel Schiff bases derived from metronidazole. *Med. Chem. Res.*, 2014, 23(11), 4872-4882.
16. Al-Zuhairi MI, Shakya AK, Numan NA, Al-Tameemi SJ, Al-Qazzan MB. Evaluating the activity of *Momordica charantia* (bitter gourd) fruit and *Curcuma longa* (turmeric) rhizome extract as anti-hyperlipidemic agents in experimental animals. *Int. J. Drug Delivery Technol.*, 2025, 15(3), 1101-1108.
17. Johansen M, Larsen C. A comparison of the chemical stability and the enzymatic hydrolysis of a series of aliphatic and aromatic ester derivatives of metronidazole. *Int. J. Pharm.*, 1985, 26(3), 227-241.
18. Li HQ, Xiao ZP, Fang RQ, Zhu HL. The syntheses and crystal structures of metronidazole-derived compounds. *J. Chem. Crystallogr.*, 2008, 38(6), 461-466.
19. Pi WX, Yang YM, Li HQ, Zhu HL. Chlorometronidazole. *Struct. Rep.*, 2005, 61(9), o2880-o2881.
20. Mokhtar Z, Eissa ME, Al-Qazzan MB, Kasabri V, Al-Akeedi M, Awad SH, Yousef TA, Al-Karmalawy AA. Synthesis, characterization, molecular modelling, and antimicrobial evaluation of novel drug–polymer composites grafted with polyvinylpyrrolidone. *J. Mol. Struct.*, 2026, 145842.
21. Hossain TJ. Methods for screening and evaluation of antimicrobial activity: A review of protocols, advantages, and limitations. *Eur. J. Microbiol. Immunol.*, 2024, 14(2), 97-115.
22. Al-Akeedi M, Najdawi M, Al-Balas Q, Al-Qazzan MB, Telfah ST. Novel anthraquinone amide derivatives as potential glyoxalase-I inhibitors. *J. Med. Life*, 2024, 17(1), 87-98
23. Al-Qazzan M, Al-Balas Q, Alnajjar B, Al-Akeedi M. Discovery of hydroxytriazole as a potential glyoxalase-I inhibitor utilizing computer-aided drug design techniques. *Sci. Rep.*, 2026.
24. Mokhtar Z, Ali AJ, Awad SH, Bashar M, Al-Qazzan MA. Preparation of new Schiff base derivatives from chitosan grafted with polyvinylpyrrolidone and study of their antimicrobial activity. *Trop. J. Pharm. Res.*, 2025, 24(7), 935-948.
25. Al-Qazzan M, Al-Balas Q, Alnajjar B, Kasabri V, Al-Hiari Y, Zayed A, AlKhateeb R, Al-Akeedi M. Cytotoxic, anti-inflammatory, antioxidant, and anti-glyoxalase-I evaluation of chelating substances: *In silico* and *in vitro* study. *PLoS One*, 2025, 20(10), e0333405.
26. Alzghoul M, Al-Hiari Y, Kasabri V, Hamdan I, Arabiyat S, Al-Balas Q, AlQazzan MB, AlSaad D, Telfah A. Unique bidentate chelators of functionalized heterocyclic fluoroquinolones with dual anti-inflammatory and selective cytotoxic effects via a C7-C8 ethylene diamine bridge. *Curr. Med. Chem*., 2026.
27. Busari HK, Azeez LA, Aremu HK, Ayinla SO, Jinadu LA, Obaleye JA. Zinc and copper complexes of 4-methylbenzoic acid and 2-methylimidazole: Synthesis, character-ization, antimicrobial and molecular docking studies. *Chemist*, 2023, 94(2).